

# Boundary layer on the surface of a neutron star

N. Babkovskaia,<sup>1,2\*</sup> A. Brandenburg<sup>2</sup> and J. Poutanen<sup>1</sup>

<sup>1</sup>*Astronomy Division, Department of Physical Sciences, University of Oulu, PO Box 3000, FIN-90014 Oulu, Finland*

<sup>2</sup>*NORDITA, Roslagstullsbacken 23, AlbaNova University Centre, 106 91 Stockholm, Sweden*

Accepted 2008 February 12. Received 2008 January 29; in original form 2007 November 16

## ABSTRACT

In an attempt to model the accretion on to a neutron star in low-mass X-ray binaries, we present 2D hydrodynamical models of the gas flow in close vicinity of the stellar surface. First, we consider a gas pressure-dominated case, assuming that the star is non-rotating. For the stellar mass we take  $M_{\text{star}} = 1.4 \times 10^{-2} M_{\odot}$  and for the gas temperature  $T = 5 \times 10^6$  K. Our results are qualitatively different in the case of a realistic neutron star mass and a realistic gas temperature of  $T \simeq 10^8$  K, when the radiation pressure dominates. We show that to get the stationary solution in a latter case, the star most probably has to rotate with the considerable velocity.

**Key words:** accretion, accretion discs – hydrodynamics – stars: neutron.

## 1 INTRODUCTION

Low-mass X-ray binaries (LMXBs) are luminous X-ray sources composed of a late-type optical companion (mass less than about  $1 M_{\odot}$ ) and a neutron star. About 100 LMXBs are known now. Neutron stars in such objects are most probably old and have a rather weak magnetic field so that an accretion disc can extend down to the neutron star surface. The rapidly rotating gas is decelerating due to viscous friction. The gas then spreads over the stellar surface and forms a boundary layer. Here most of the energy is emitted in the form of X-rays, whilst its amount is comparable with the energy generated in the accretion disc (Sunyaev & Shakura 1986; Sibgatullin & Sunyaev 1998).

LMXBs can be divided into two different classes. Very luminous Z-sources ( $L \sim 0.1-1 L_{\text{edd}}$ ) have relatively soft, two-component spectra, while both components can be approximated by black bodies with colour temperatures of about 1 and 2.5 keV, respectively (Gilfanov, Revnivtsev & Molkov 2003). The other less luminous sources ( $L \sim 0.01-0.05 L_{\text{edd}}$ ) are observed in two states: the high/soft and low/hard states. The radiation spectra in the soft state are similar to those of the Z-sources, while in the hard state they are close to the spectra of the Galactic black holes in the hard states (Barret et al. 2000).

The soft component can be associated with the radiation from the accretion disc, while the hard one is produced in the boundary layer (Mitsuda et al. 1984; Gilfanov et al. 2003). On the other hand, the spectra from the spreading layer depend on the neutron star compactness (mass/radius ratio), which determines the gravitational field at the surface. Therefore, one can get independent constraints on the equation of state of the matter at extreme densities, calcu-

lating the spectra and comparing them with the observational data (Suleimanov & Poutanen 2006).

A study of the motion of the matter very close to the neutron star is also important for understanding the production of quasi-periodic oscillations (QPOs) observed in the kHz range from a number of accreting neutron stars in LMXBs (van der Klis 2000). These QPOs may provide direct ways of measuring effects that are unique to the strong gravitational field regime. However, the question about the nature of QPOs is still open, partly because of the complexity of hydrodynamical flows in close vicinity of a neutron star surface. Thus, detailed studies of the structure of the boundary layer play the key role in understanding the physics in the vicinity of a compact object.

The first model of the boundary layer was proposed by Pringle (1977), who considers it as part of the accretion disc. In his model the gas is moving parallel to the disc mid-plane and is decelerating due to differential rotation and viscous forces. The effective temperature of the boundary layer appears to be higher than the maximum accretion disc temperature, because the size of the BL is smaller than that of the disc, whereas their luminosities are comparable. Popham & Narayan (1992) identified non-physical aspects of the standard  $\alpha$ -viscosity prescription and developed a more physically realistic model of viscosity. Narayan & Popham (1993) proposed a self-consistent model of a boundary layer on the surface of a white dwarf and accounted for the hard X-rays observed in cataclysmic variables. Medvedev (2004) studied the radiative accretion on to a rapidly spinning neutron star. They considered a quasi-spherical hot settling accretion flow and presented an analytical self-similar solution describing the boundary layer.

Inogamov & Sunyaev (1999) considered the boundary layer as a spreading layer on the surface of the neutron star. They proposed that matter spirals along the neutron star surface towards the poles due to turbulent friction between matter and stellar surface. They used a 1D approach, averaging all values in the radial direction and

\*E-mail: nbabkovs@nordita.org

assuming azimuthal symmetry. To describe the turbulent viscosity they used the Prandtl–Karman universal logarithmic dependence of the mean velocity on the distance from the stellar surface and introduced a turbulent viscosity to characterize turbulent velocity and turbulent pressure fluctuations. They also assumed that the dissipation of rotational kinetic energy causes a strong energy release near the bottom of the boundary layer. With these simplifications they constructed a semi-analytical model and showed that the kinetic energy of the gas is mostly liberated in two belts above and below the equator of the neutron star.

In order to solve the 1D spreading layer problem, Inogamov & Sunyaev (1999) assumed that the initial rotational velocity in the equatorial plane is very close to Keplerian. However, because of the presence of the boundary layer associated with the accretion disc, this velocity can significantly deviate from the Keplerian value. There is no doubt that the behaviour of the gas at higher latitudes in the spreading layer strongly depends on the conditions in the equatorial plane. Therefore it is important to describe the gas flow near the equatorial point more accurately. As a first step we present here 2D numerical hydrodynamic solutions in the neighbourhood of the equatorial point.

## 2 EQUATIONS AND COORDINATES

The full non-stationary system of the hydrodynamical equations is as follows. The continuity equation is solved in the form

$$\frac{D \ln \rho}{Dt} = -\nabla \cdot \mathbf{U}, \quad (1)$$

where  $\rho$  and  $\mathbf{U}$  are density and velocity of the gas, and  $D/Dt = \partial/\partial t + \mathbf{U} \cdot \nabla$  is the advective derivative. The conservation of momentum can be written in the form

$$\frac{D\mathbf{U}}{Dt} = -\frac{1}{\rho}\nabla p + \mathbf{F}_{\text{gr}} + \mathbf{F}_{\text{vs}} + \frac{\kappa \mathcal{F}_{\text{rad}}}{c}, \quad (2)$$

where  $\mathbf{F}_{\text{gr}} = -GM_{\text{star}}\mathbf{r}/r^3$  is the gravitational force (where  $M_{\text{star}}$  is a stellar mass,  $\mathbf{r}$  is a radius vector),  $\mathbf{F}_{\text{vs}} = \rho^{-1} \nabla \cdot (2\nu_t \mathbf{S})$  is the viscous force,  $\nu_t$  is the turbulent viscosity,  $\mathcal{F}_{\text{rad}}$  is a radiative flux,  $\kappa$  is the opacity and  $c$  is the speed of light. The energy equation is formulated in terms of specific entropy  $s$ ,

$$T \frac{Ds}{Dt} = 2\nu_t \mathbf{S}^2 - \frac{1}{\rho} \nabla \cdot \mathcal{F}_{\text{rad}}, \quad (3)$$

where  $T$  is the temperature and  $\mathbf{S} = (1/2)(U_{i,j} + U_{j,i}) - (1/3)\delta_{ij} \nabla \cdot \mathbf{U}$  is the traceless rate of strain tensor and commas denote partial differentiation. In the following we assume that the gas is optically thick and can therefore treat radiation in the diffusion approximation, so the radiative flux is given by

$$\mathcal{F}_{\text{rad}} = -K \nabla T, \quad (4)$$

where  $K = 16\sigma_{\text{SB}}T^3/(3\kappa\rho)$  is the radiative conductivity.

A sketch of the boundary layer on the surface of the neutron star is presented in Fig. 1. The gas is accreting in the disc mostly in the radial direction  $R$  and turns in the  $Z$  direction near the equatorial point  $E$ . Since the purpose of this paper is to study the gas flow in the vicinity of  $E$ , we use cylindrical coordinates, and neglect the curvature of the stellar surface. We consider a 2D domain limited in the radial direction by the surface of the star and the disc zone, where the rotational velocity  $U_\phi$  is close to the Keplerian value  $U_K$  (see Fig. 2).

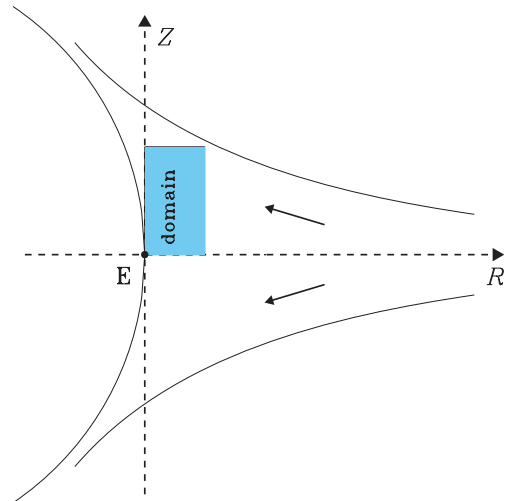


Figure 1. Sketch of the boundary layer on the surface of the neutron star.

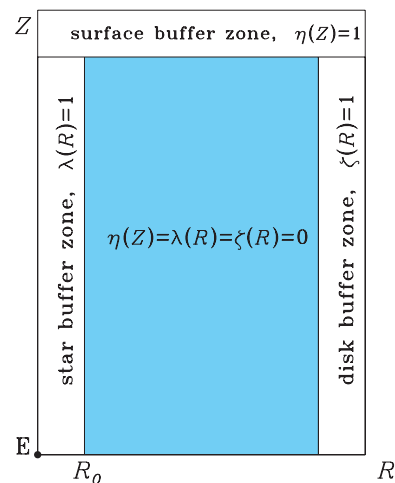


Figure 2. Sketch of the calculated domain and of the buffer zones.

## 3 BOUNDARY CONDITIONS AND BUFFER ZONES

The boundary conditions represent an integral part of the overall solution in that the values on the boundaries both determine and depend themselves on the final solution. They must allow the accretion on to the stellar surface and the emission of energy. They must also simulate the compression of gas near the surface and allow this gas to become part of the surface, while the gas settling depends itself on the input parameters of incoming gas and conditions on the stellar surface. The rotational velocity of the gas in the disc part is close to Keplerian, but cannot be exactly Keplerian, because otherwise accretion would stop and the boundary layer would disappear. On the other hand, the deviation from the Keplerian velocity is determined by the conditions on the stellar surface. To cope with these complications we use so-called buffer zones, which are narrow regions just outside the domain (of the size of typically five grid points; see Fig. 2), where additional terms are added to the hydrodynamical equations. This type of approach has proven to be useful in earlier simulations of disc outflows and star–disc coupling (von Rekowski et al. 2003). We use three different buffer zones that are characterized by the three profile functions  $\zeta(R)$  for the disc buffer zone,

**Table 1.** Parameters.

Quantity	Case 1	Case 2
$R_{\text{star}}$	$10^6$ cm	$10^6$ cm
$M_{\text{star}}$	$1.4 \times 10^{-2} M_{\odot}$	$1.4 M_{\odot}$
$T_{\text{star}}$	$3 \times 10^6$ K	$10^8$ K
$T_{\text{disc}}$	$1.5 \times 10^6$ K	$10^8$ K
$\rho_{\text{disc}}(0)$	$0.1 \text{ g cm}^{-3}$	$4 \text{ g cm}^{-3}$
$\nu_t$	$10^7, 10^8 \text{ cm}^2 \text{ s}^{-1}$	$10^{10} \text{ cm}^2 \text{ s}^{-1}$
$\alpha$	0	1

$R_{\text{star}}$  is a stellar radius,  $M_{\text{star}}$  is stellar mass,  $T_{\text{star}}$  and  $T_{\text{disc}}$  are temperatures of the star surface and the gas in the disc zone,  $\rho_{\text{disc}}(0)$  is the gas density at the mid-plane in the disc zone,  $\nu_t$  is a turbulent viscosity.

$\lambda(R)$  for the star buffer zone, and  $\eta(Z)$  for the surface buffer zone. In the following we describe the properties of these three zones separately.

In the disc buffer zone, where  $\zeta(R) = 1$ , the gas is accelerated close to the Keplerian speed due to an additional source term in the equation for  $U_{\phi}$ , while  $U_R$  adjusts itself to the conditions inside the domain. Thus, the  $\phi$  and  $R$  components of equation (2) are modified by additional terms on their right-hand sides,

$$\frac{DU_{\phi}}{Dt} = \dots - \frac{U_{\phi} - U_K(R)}{\tau} \zeta(R), \quad (5)$$

$$\frac{DU_R^j}{Dt} = \dots - \frac{U_R^j - U_R^{j-1}}{\tau} \zeta(R), \quad j = 1, \dots, N_R, \quad (6)$$

where  $j$  denotes the meshpoint in the  $R$  direction,  $N_R$  is total number of the grid points in the  $R$  direction, and dots indicate the presence of terms that were already specified in equation (2). We take  $\tau = 5\delta t$ , where  $\delta t$  is the length of the time-step.

In the buffer zone near the star, where  $\lambda(R) = 1$ , the radial gas velocity goes down to zero at the stellar surface. To describe the rotation of the star we introduce the parameter  $0 \leq \alpha \leq 1$ , which equals zero if the star is non-rotating one, and unity if it rotates with the corresponding Keplerian velocity. Thus the  $\phi$  and  $R$  components of equation (2) are modified further by the terms

$$\frac{DU_{\phi}}{Dt} = \dots - \frac{U_{\phi} - \alpha U_K}{\tau} \lambda(R), \quad (7)$$

$$\frac{DU_R}{Dt} = \dots - \frac{U_R}{\tau} \lambda(R), \quad (8)$$

where  $\lambda(R) = 1$  in the buffer zone, and zero outside.

The surface buffer zones will be discussed separately in the following two sections, because they have to be treated differently for gas and radiation pressure-dominated regimes.

The temperatures on the stellar surface and the disc (left- and right-hand boundaries of the domain) are fixed by  $T_{\text{star}}$  and  $T_{\text{disc}}$ , respectively, while the gas density is extrapolated on both sides. On the lower boundary of the domain (mid-plane of the disc) we use antisymmetric boundary conditions for the  $Z$  component of the velocity and symmetric boundary conditions for all other quantities, while on the upper domain boundary all quantities are extrapolated. The turbulent viscosity  $\nu_t$  is assumed to be constant everywhere in the domain.

For all simulations presented here we use the PENCIL CODE,<sup>1</sup> which is a high-order finite-difference code (sixth order in space and third

order in time) for solving the compressible hydrodynamic equations (Brandenburg & Dobler 2002).

#### 4 GAS PRESSURE-DOMINATED CASE

As a first test we consider a gas pressure-dominated case and choose the gas temperature in the disc to be  $T_{\text{disc}} = 1.5 \times 10^6$  K. This means that the radiation pressure is about two orders of magnitude smaller than the gas pressure. Also, we take the stellar mass to be  $M_{\text{star}} = 10^{-2} M_{\odot}$  so as to balance the gravity force near the surface by the gas pressure force. In addition, we assume that the star does not rotate ( $\alpha = 0$ ). We consider two cases with  $\nu_t = 10^7$  and  $10^8 \text{ cm}^2 \text{ s}^{-1}$  (see Table 1).

Since initially the disc is assumed to be in vertical hydrostatic equilibrium, the vertical velocity should be close to zero. In addition, we let the gas density  $\rho$  approach a certain vertical profile  $\rho_{\text{disc}}(Z)$ , where the value at the disc mid-plane is  $\rho_{\text{disc}}(0) = 0.1 \text{ g cm}^{-3}$ , and assume that  $\rho$  decreases exponentially with  $Z$ . However, since the temperature profile results from a thermal balance between viscous heating and radiative cooling, the local sound speed  $c_s$  in equation (9) is recalculated at each time-step. This allows the vertical density profile to adjust to the conditions inside the domain. Thus, we have in the disc buffer zone

$$\frac{D \ln \rho}{Dt} = \dots - \frac{\ln \rho - \ln \rho_{\text{disc}}}{\tau} \zeta(R), \quad (9)$$

$$\frac{DU_Z}{Dt} = \dots - \frac{U_Z}{\tau} \zeta(R), \quad (10)$$

where

$$\rho_{\text{disc}}(Z) = \rho_{\text{disc}}(0) \exp\left(-\frac{Z^2}{2H^2}\right) \quad \text{and} \quad \frac{1}{H^2} = \frac{\gamma G M_{\text{star}}}{R^3 c_s^2}, \quad (11)$$

where  $\zeta(R) = 1$  in the disc buffer zone, and zero outside.

In the surface buffer zone, where  $\eta(Z) = 1$ , we assume vanishing first derivatives for all three velocity components  $U_i$  ( $i = 1, \dots, 3$ ) and for the specific entropy. We also correct the density profile to account for the resulting artificial pressure force which works against the vertical gravity. Due to this term, the gas flows out through the surface boundary rather than coming into the domain at the beginning of the calculation. Thus, we add the terms

$$\frac{D \ln \rho^j}{Dt} = \dots - \frac{\ln \rho^j - \ln \rho^{j-1} + Z^2/(2H^2)}{\tau} \eta(Z_{j-1}), \quad (12)$$

$$\frac{DU_i^j}{Dt} = \dots - \frac{U_i^j - U_i^{j-1}}{\tau} \eta(Z_j), \quad (13)$$

$$\frac{DS^j}{Dt} = \dots - \frac{s^j - s^{j-1}}{\tau} \eta(Z_j), \quad j = 1, \dots, N_R. \quad (14)$$

We consider two runs with  $\nu_t = 10^7$  and  $10^8 \text{ cm}^2 \text{ s}^{-1}$  and show in Fig. 3 two cross-sections respectively for  $R - R_{\text{star}} = 1.25$  and 2 m,  $\nu_t = 10^7$  and  $10^8 \text{ cm}^2 \text{ s}^{-1}$ , and  $Z = 5$  m in both cases. In Fig. 4 we show velocity and density. One can see that the accreting gas comes to the stellar surface and turns towards the poles of the neutron star.

We find that the size of the boundary layer, where the rotational velocity  $U_{\phi}$  of the gas decreases from the Keplerian value down to zero, strongly depends on the value of the turbulent viscosity. The boundary layer becomes 3.5 times thicker if one increases  $\nu_t$  by a factor of 10. This is consistent with the classical theory of a boundary layer, according to which the thickness of the boundary

<sup>1</sup> <http://www.nordita.dk/software/pencil-code>.

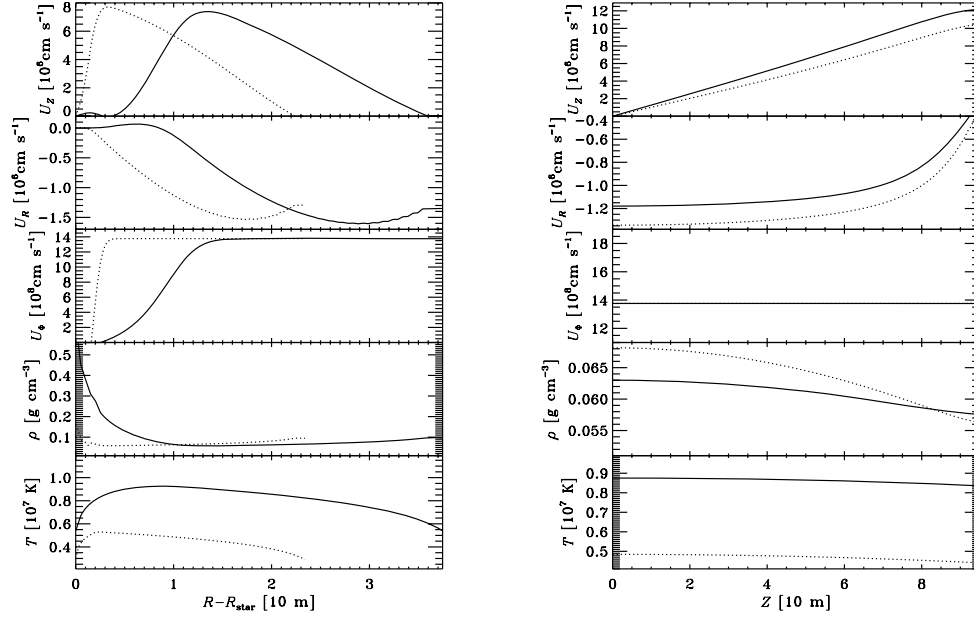


**Figure 3.** Gas velocity, density and temperature as a function of  $R$  and  $Z$  for the gas pressure-dominated case ( $M_{\text{star}} = 1.4 \times 10^{-2} M_{\odot}$ ). The dotted and solid lines correspond to  $\nu_t = 10^7$  and  $10^8 \text{ cm}^2 \text{ s}^{-1}$ , respectively. Left-hand panel: fixed  $Z = 50 \text{ m}$ , right-hand panel: fixed  $R - R_{\text{star}} = 12.5 \text{ m}$  for  $\nu_t = 10^7$  and  $R - R_{\text{star}} = 20 \text{ m}$  for  $\nu_t = 10^8 \text{ cm}^2 \text{ s}^{-1}$  cases.

layer is inversely proportional to the square root of the Reynolds number,  $\sqrt{Re} \sim 1/\sqrt{\nu_t}$  (see e.g. Shih-I Pai 1962). The increase of viscosity also leads to a growth of the gas temperature, resulting from a balance between turbulent viscous friction and radiative cooling. One can see that the temperature achieves its maximal value in the middle of the boundary layer, where the velocity gradient and therefore the heating rate are maximum.

Note that the solution for our test case looks similar to the spreading layer model for the white dwarf case. We find that the  $Z$  component of the gas velocity  $V_Z = 10^6 \text{ cm s}^{-1}$  is very close to that obtained by Piro & Bildsten (2004). Unfortunately, we cannot compare other quantities because the values in the spreading layer model are averaged along the  $R$  direction.

## 5 RADIATION PRESSURE-DOMINATED CASE

Let us now consider a realistic neutron star mass,  $M_{\text{star}} = 1.4 M_{\odot}$ . We find that, in order to balance the gravity force by the gas pressure gradient near the stellar surface, the gas temperature must attain a value of  $3 \times 10^{12} \text{ K}$ , which is unrealistic. Therefore, in the case of a non-rotating star, the only force which can work against gravity is the radiation pressure gradient. Indeed, if one takes the gas temperature to be  $T = 3 \times 10^8 \text{ K}$  and  $\rho \gtrsim 0.3 \text{ g cm}^{-3}$ , the radiation pressure force becomes comparable to the gravitational force (i.e.  $GM_{\text{star}}/R^2 \lesssim \sigma_{\text{SB}} T_{\text{star}}^4/(c\rho)$ , where  $\sigma_{\text{SB}}$  is the Stefan–Boltzmann constant).

Using standard disc theory, we estimate the turbulent viscosity near the stellar surface  $\nu_t = \alpha_d H c_s \simeq 10^{10} \text{ cm}^2 \text{ s}^{-1}$ , where  $\alpha_{\text{disc}} \simeq 0.01$  is a viscosity parameter,  $H \simeq 0.01 R_{\text{star}}$  and  $c_s \simeq 10^8 \text{ cm s}^{-1}$ . Note that the radiative viscosity  $\nu_r = 4\sigma_{\text{SB}} T^4 m_p / (\kappa c^2 \rho) \simeq 10^8 \text{ cm}^2 \text{ s}^{-1}$  (where  $m_p$  is a proton mass) is much smaller than the turbulent one, and can be neglected.

We find that the description of buffer zones must be modified in the radiation pressure-dominated case. For simplicity we use a similar density profile in the disc buffer zone as it was in the gas pressure-dominated case. However, we now take  $\rho_{\text{disc}}(0) = 4 \text{ g cm}^{-3}$

and fix the gas temperature  $T_{\text{disc}}$  to avoid large radiation pressure gradients and therefore the generation of large velocities, which lead to strongly non-stationary behaviour in the buffer zone and eventually to numerical instability. Also, we use a softer condition for the  $Z$ -velocity by assuming vanishing first derivatives. Thus, we set

$$\frac{D \ln \rho}{Dt} = \dots - \frac{\ln \rho - \ln \rho_{\text{disc}}}{\tau} \zeta(R), \quad (15)$$

$$\frac{DU_Z^j}{Dt} = \dots - \frac{U_Z^j - U_Z^{j-1}}{\tau} \zeta(R), \quad j = 1, \dots, N_R \quad (16)$$

$$\frac{Ds}{Dt} = \dots - \frac{T/T_{\text{disc}} - 1}{\tau} \zeta(R). \quad (17)$$

In the course of the calculation we find that inside the domain cold low-density patches surrounded by denser hot gas appear sporadically. Such patches are dispersed due to motion of the gas from the core of the patch outward through the radiation pressure gradient. However, if we were to fix the  $Z$  and  $R$  velocities in the star buffer zone to zero, such a patch cannot disappear, while the density inside this patch is going to decrease together with the temperature, and a numerical instability develops. To avoid this we use symmetry conditions relative to the inner boundary of the buffer zone  $R = R_0$  (see Fig. 2) for  $\ln \rho, s$  and  $U_Z$ . In addition we assume  $U_Z = 0$  at  $R = R_0$ . Thus, we have in the star buffer zone

$$\frac{D \ln \rho(R)}{Dt} = \dots - \frac{\ln \rho(R) - \ln \rho(2R_0 - R)}{\tau} \lambda(R), \quad (18)$$

$$\frac{DU_Z(R)}{Dt} = \dots - \frac{U_Z(R) - U_Z(2R_0 - R)}{\tau} \lambda(R), \quad (19)$$

$$\frac{Ds(R)}{Dt} = \dots - \frac{s(R) - s(2R_0 - R)}{\tau} \lambda(R). \quad (20)$$

Since the main goal of this paper is to consider the gas flow in the vicinity of the equatorial point  $E$ , we consider a domain located

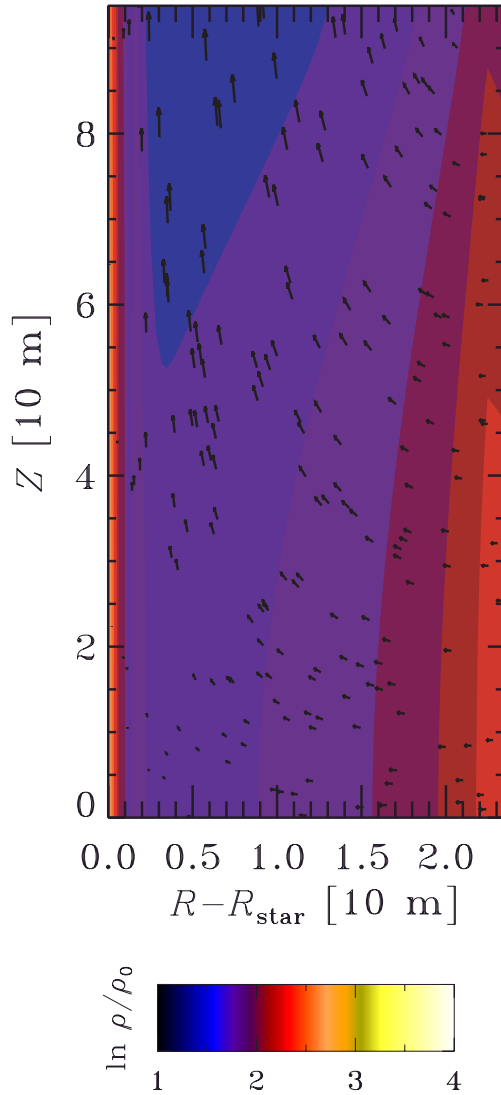


**Figure 4.** Density and velocity fields in a vicinity of a star in a gas pressure-dominated case ( $M_{\text{star}} = 1.4 \times 10^{-2} M_{\odot}$ ). The domain is limited in the radial direction by the surface of a neutron star and in the disc mid-plane. The surface and disc buffer zones are excluded. The viscosity is  $\nu_t = 10^7 \text{ cm}^2 \text{ s}^{-1}$ , the density scale is  $\rho_0 = 10^{-2} \text{ g cm}^{-3}$ .

inside the disc with a vertical size smaller than the height where the gas becomes cold and optically thin. To imitate a disc photosphere in the surface buffer zone we include an additional cooling term to create a vertical temperature gradient and to allow gas to escape through the surface boundary.

First, we attempt to consider a non-rotating star. It turns out that in this case the initial distribution of the main quantities (temperature, density and velocity) have to be close to the final state, because otherwise inhomogeneities in the temperature result in large radiation pressure gradients which, in turn, generate large local velocities. Such velocity perturbations may produce a local decrease of density, which will lead to a decrease in radiative cooling, and hence to an increase in temperature. The resulting radiation pressure gradient will decrease the density even further, which leads therefore to an instability. (Note that this does not happen in the case of a smaller gas temperature because then the gas pressure dominates over the radiation pressure.)

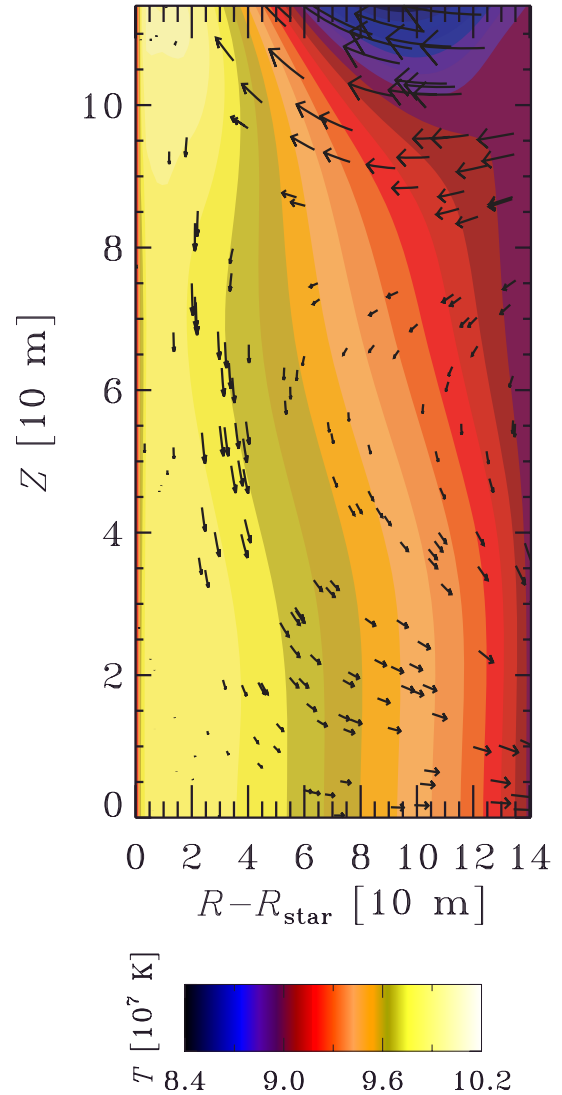


**Figure 5.** Temperature and velocity fields in a vicinity of a neutron star in a radiation pressure-dominated case ( $M_{\text{star}} = 1.4 M_{\odot}$ ). The domain is the same as in Fig. 4 for  $\nu_t = 10^{10} \text{ cm}^2 \text{ s}^{-1}$ .

Finding suitable initial conditions is a difficult task. It turns out that it is easier to consider first a rotating star, and then to decrease its rotational velocity down to the necessary value. However, the final rotational velocity still has to be considerable so that centrifugal and gravitational forces are of the same order of magnitude. In the opposite case, i.e. when the star is almost non-rotating, the gravity force has to be balanced by the radiation pressure gradient, which, in turn, should be negative near the stellar surface. However, it is not clear how to realize this, because the main heating mechanism is due to viscous friction which is maximum in the middle of the boundary layer rather than at the stellar surface.

At the current stage we assume that the rotational velocity of the star corresponds to the Keplerian velocity at the stellar radius (i.e.  $\alpha = 1$ ). All other parameters are presented in Table 1. Also, we take a uniform initial distribution of temperature in the  $R$  direction. In that case, at the beginning of the calculation, the huge gravitational force near the stellar surface is balanced by the centrifugal force. Depending on the temperature gradient, the  $R$  component of the radiation

pressure force nearly vanishes and the resulting  $R$  component of the velocity appears to be small.

While the  $Z$  component of the gravitational force is much smaller than the  $R$  component, its influence on the gas motion in the  $Z$  direction is crucial and leads to strong flow of gas into the domain through the surface boundary and to an accumulation of gas near the equatorial point  $E$ . To avoid numerical problems, we assume that initially the  $Z$  component of gravitational force is balanced by the corresponding component of the radiation pressure force. Therefore, the initial distribution of temperature takes the form

$$T(R_i) = T(R_{i-1}) - \frac{3GM_{\text{star}}c\rho(R_i)Z_i}{16\sigma_{\text{SB}}R_i^3T^3(R_i)}\Delta R, \quad i = 1, \dots, N_R, \quad (21)$$

where  $\Delta R$  is the size of the mesh in the  $R$  direction. We use the same initial density distribution as in the gas pressure-dominated case (see Section 4).

In Fig. 5 we present temperature and velocity fields (see also the sketch in Fig. 1). Here we show temperature rather than density (as was done in Fig. 4), because in the radiation pressure-dominated case the flow of the gas is mostly determined by the radiation pressure force and hence by the temperature distribution. In addition, we take a larger domain size because the thickness of the boundary layer now appears to be an order of magnitude larger than that in Section 4.

The results of the calculation are also presented in Fig. 6, where density, temperature and velocity of the gas are shown as functions of  $R$  for three different distances from the mid-plane,  $Z = 10, 50$  and  $110$  m. We find that at higher latitudes the gas rotates with a velocity that is comparable to the rotational velocity of the star, while in the equatorial plane its rotational velocity is smaller than the stellar surface speed. This means that in the equatorial plane the centrifugal force is larger than the gravitational force, while at the higher latitudes the centrifugal force is smaller than the gravitational force.

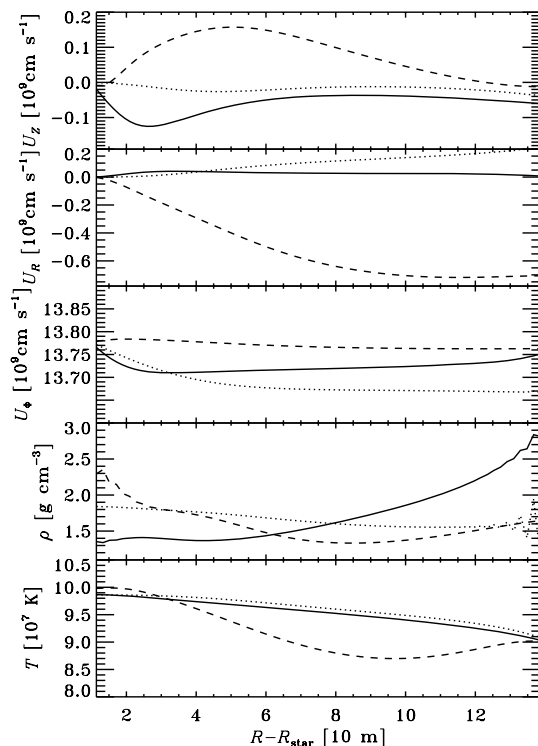


**Figure 6.** Gas velocity, density and temperature as a function of  $R$  for the fixed  $Z = 10$  m (dotted curve),  $Z = 50$  m (solid curve) and  $Z = 110$  m (dashed curve). The star buffer zone is excluded.

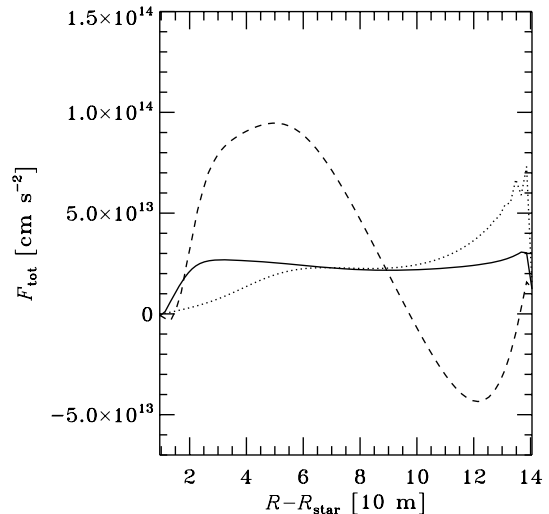


**Figure 7.** The sum of the gravitational, centrifugal and radiation pressure forces in the  $R$  direction as a function of  $R$  for values of  $Z$  as in Fig. 6.

Such a relation between the main forces would result in accretion in the equatorial plane and excretion at higher latitudes, provided the gas pressure was much larger than the radiation pressure. However, since now the radiation pressure dominates, we obtain the opposite result: the gas accretes only at higher latitudes, while in the equatorial plane it is excreting.

In Fig. 7 we present, as a function of  $R$ , the sum of the  $R$  components of gravitational, centrifugal and radiation pressure forces,  $F_{\text{tot}} = F_{\text{gr}} + U_{\Phi}^2/R + \kappa \mathcal{F}_{\text{rad}}/c$ . One can see that at a higher latitudes the total force is at some radius negative,  $F_{\text{tot}} < 0$ , so the generated radial velocity is negative ( $U_R < 0$ ), which means accretion, while in the equatorial plane  $F_{\text{tot}} > 0$  and  $U_R > 0$ , so the gas is excreting. The dominant role of the radiation pressure in driving the velocity field is also clear from analysing the temperature in Fig. 5. One can see that the temperature decreases outward in the equatorial plane and increases outward at  $Z \simeq 110$  m near the disc buffer zone. Note that along the stellar surface the temperature is almost constant, so the  $Z$  component of the gravitational force dominates here, and causes the gas to sink towards the equatorial plane.

## 6 CONCLUSIONS

We have studied the gas flow in close vicinity of a neutron star in an LMXB and have assumed that the magnetic field is negligible. The main purpose of this work was to investigate the flow near the equatorial plane between disc and star, so the curvature of the stellar surface in the latitudinal direction was neglected and cylindrical coordinates were used.

In the unrealistic, gas pressure-dominated case the gas temperature is  $T \simeq 5 \times 10^6$  K (which is about an order of magnitude smaller than the observed value). If the star does not rotate, the gravitational force at a radius close to the stellar surface should be balanced by the gas pressure force. To have gas pressure and gravitational forces of the same order of magnitude, the stellar mass was chosen to be about two orders of magnitude smaller than the real mass of a neutron star. In this case the maximum release of energy occurs in the middle of the boundary layer, where the gas velocity gradient (and hence the viscous heating) reaches a maximum, while the radiation pressure force at the stellar surface is directed inward.

For a realistic neutron star mass,  $M_{\text{star}} = 1.4 M_{\odot}$ , the gas pressure gradient at the stellar surface becomes negligible compared with the gravitational force. The latter is balanced by the radiation pressure, so the gas temperature is about  $T \simeq 10^8$  K. Unlike the gas pressure-dominated case, the radiation pressure force is directed outward rather than inward. Thus, the maximum energy release occurs directly at the stellar surface. However, it is not clear how to realize such a scenario, where the gas is heated by viscous friction between the differentially rotating gas layers.

The picture becomes crucially different if one considers a rotating neutron star: the gravitational force can now be balanced by the centrifugal force. Here we have assumed that the neutron star rotates with the Keplerian velocity at the stellar radius. Alternatively, one might find a solution for smaller rotational velocities by gradually decreasing it down to the required value, using the result of calculating it for a larger velocity as an initial approximation for calculation with the smaller value.

We find that at higher latitudes the centrifugal force is larger than the gravitational force, while at the equatorial plane the gas rotates with a velocity that is considerably smaller than the corresponding Keplerian value. It would be reasonable to assume that the gas is accreting near the equator and excreting at higher latitudes. However, we find the opposite: the accretion occurs only at higher latitudes, while in the equatorial plane the gas is excreting. This is related to the temperature distribution, and therefore, to the radiation pressure force, which is now dominant. We find that near the equatorial plane the temperature decreases outward, so the gas is pushed away from the surface by radiation pressure. At higher latitudes, some distance away from the surface, the temperature decreases inward, resulting in accretion. The circulation of the gas is closed by a flow along the stellar surface from high to low latitudes, because the temperature is almost constant in this direction and the gas flow is controlled only by the tangential component of gravity.

Finally, one should note that, since we have considered only a laminar 2D model of the boundary layer at the neutron star surface, we have assumed that the turbulent viscosity is constant everywhere and that it can be treated as an input parameter. Future 3D simulations will allow us to model turbulent processes more accurately.

However, even the results of the 2D simulations give us some clues for understanding the physical processes near the neutron star surface. These results can in principle be used for a more detailed description of the vertical structure of the boundary layer and for calculating spectra of neutron star radiation. Furthermore, the presented results may be useful for understanding the nature of QPOs.

## ACKNOWLEDGMENTS

This work was supported by the Academy of Finland grant 110792 and the Magnus Ehrnrooth Foundation. We acknowledge the allocation of computing resources provided by the Centre for Scientific Computing in Finland.

## REFERENCES

- Barret D., Olive J. F., Boirin L., Done C., Skinner G. K., Grindlay J. E., 2000, *ApJ*, 533, 329  
 Brandenburg A., Dobler W., 2002, *Comput. Phys. Commun.*, 147, 471  
 Gilfanov M., Revnivtsev M., Molkov S., 2003, *A&A*, 410, 217  
 Inogamov N. A., Sunyaev R. A., 1999, *Astron. Lett.*, 25, 269  
 Medvedev, 2004, *ApJ*, 613, 506  
 Mitsuda K. et al., 1984, *PASJ*, 36, 741  
 Narayan R., Popham R., 1993, *Nat*, 362, 820  
 Piro A. L., Bildsten L., 2004, *ApJ*, 610, 977  
 Popham R., Narayan R., 1992, *ApJ*, 394, 255  
 Pringle J. E., 1977, *MNRAS*, 178, 195  
 Shih-I Pai, 1962, *Introduction to the Theory of Compressible Flow*. Van Nostrand, Princeton  
 Sibgatullin N. R., Sunyaev R. A., 1998, *Astron. Lett.*, 24, 774  
 Suleimanov V., Poutanen J., 2006, *MNRAS*, 369, 2036  
 Sunyaev R. A., Shakura N. I., 1986, *Sov. Astron. Lett.*, 12, 117  
 van der Klis M., 2000, *ARA&A*, 38, 717  
 von Rekowski B., Brandenburg A., Dobler W., Shukurov A., 2003, *A&A*, 398, 825

This paper has been typeset from a  $\text{\TeX}/\text{\LaTeX}$  file prepared by the author.